Electron Temperature and Plasma Potential Measurements in a Radial Plasma Source

IEPC-2013-272

Presented at the 33rd International Electric Propulsion Conference,
The George Washington University • Washington, D.C. • USA
October 6 – 10, 2013

Gennady Makrinich,[1] D. Zoler,[2] and A. Fruchtman[3]
H.I.T. – Holon Institute of Technology, Holon, 58102, Israel

Abstract: The radial dependencies of the electron temperature and density and of the plasma potential in Radial Plasma Source (RPS) were measured. The plasma pressure is calculated and is compared to the pressure exerted on a balance force meter by the mixed ion-neutral flux exiting the RPS. It is concluded that the force exerted on the balance force meter is considerably larger than that resulted from the plasma pressure. This indicates that most of the force results from magnetic pressure.

Nomenclature

ϕ	=	the electric potential
T	=	the electron temperature
e	=	the elementary charge
a	=	emissive probe radius
n	=	plasma density
λ_D	=	Debye length
R_s	=	radial plasma source radius

I. Introduction

THE Radial Plasma Source (RPS) accelerates plasma and neutrals radially outward by an applied radial electric field across an axial magnetic field.[1] In a modified geometry, the RPS could be used as a thruster, somewhat similar to the Hall thruster (HT). We have shown that in the RPS, due to ion- neutral collisions, the ratio of thrust over power into the ions is very high.[1-3] The role of the ion-neutral collisions is similar to the ionic wind,[4] which relies on electric pressure. We will show elsewhere that because the RPS uses magnetic pressure, the thrust can be much larger. Here we present measurements of the radial dependencies of the electron temperature and density and of the plasma potential in the RPS. We calculate the plasma pressure and compare it to the pressure exerted on a balance force meter by the mixed ion-neutral flux exiting the RPS. We conclude that the force exerted on the balance force meter is considerably larger than that resulted from the plasma pressure. This indicates that most of the force results from magnetic pressure.

In Section II we describe the measurement method. The method was presented in a conference[6] and is described here again for completeness. In Section III we present the results of the measurements, the profiles of the plasma density, of the electron temperature, of the plasma pressure, and of the plasma potential. In Section IV we discuss the results. We conclude that the plasma-neutral flow gain most of the momentum from magnetic pressure and not from plasma pressure.

[1] Research Scientist, Faculty of Sciences, Gennady@hit.ac.il .
[2] Visiting Scientist, on leave from Soreq Nuclear Research Center, Yavne 81800, Israel, zoler@soreq.gov.il.
[3] Professor, Faculty of Sciences, fnfrucht@hit.ac.il.

II. The method of measurements

We have developed a theory of an emissive probe, that enables us to calculate the normalized electric potential, $\psi \equiv e\phi / T$, as well as the variation of plasma parameters in the vicinity of the probe. Here, ϕ is the electric potential and T the electron temperature. In all the cases we deal with here, the probe used for the potential measurements is floating. Our main interest is to know what is the normalized probe potential relative to the plasma, $\psi_c \equiv e\phi_c / T$. A characteristic parameter is the Debye number, $\delta \equiv \lambda_D / a$, where λ_D is the Debye length and a the radius of the cylindrical probe.

If the floating probe is cold and non-emitting, the probe potential is considerably lower than the plasma potential in order to repel the plasma electrons so that the ion and electron fluxes from the plasma to the probe are equal. When the floating probe is heated and emits electrons, current neutrality is partially maintained by the emitted electrons. This allows the electron current from the plasma to be larger, and the potential of the probe is closer to the plasma potential. As electron emission from the probe is increased the electric field at the probe decreases until the electric field becomes zero. This is the space charge limit and current saturation. The probe potential even then is still lower than the plasma potential, in order to draw electron current from the probe. Figure 2 shows how the potential drop between the plasma and the probe ψ_c and the three normalized currents, plasma ion and electron currents and electron current from the probe, vary when the electron emission from the probe is increased. The results are for $\delta \to 0$ and for argon plasma. The potential of the floating probe varies from $\psi_c = -5.2$, when the probe is cold and not emitting; to $\psi_c \cong -1.5$ when the probe is hot and emitting up to the space-charge limit current.

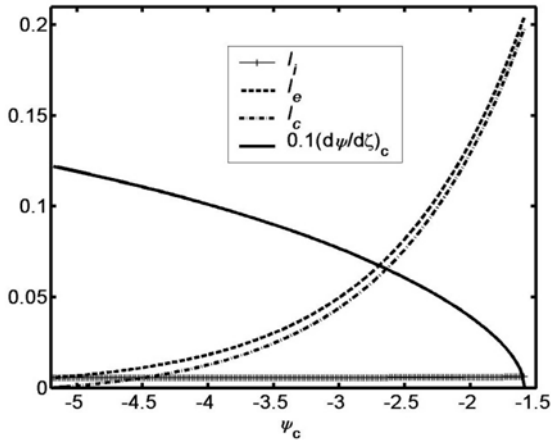

Figure 1. Variations of the probe potential relative to the plasma potential and of the currents when the probe is heated and the electron emission grows from zero to the space-charge limit of current saturation.[5]

The probe potential crucially depends on the Debye number δ. In order for the probe to emit electrons when it is heated, its radius has to be small and therefore often δ is finite. The probe potential gets closer to the plasma potential if δ is larger. The normalized potential difference between the plasma and the probe versus δ, as found in our theory,[5] is shown in Figs 2 and 2.

Figure 2 shows the probe potential relative to the plasma potential as a function of Debye number δ for a cold, non-emitting probe. When $\delta = 0$, the value of the potential coincides with the value obtained for a planar sheath. We note that in all the calculations in our model, the ions are assumed collisionless during their motion from the plasma to the probe. As is well known for the planar collisionless sheath, the potential difference when $\delta = 0$ depends logarithmically on the ion-electron mass ratio. The results in Fig. 2 are for argon plasma. The calculation for a cold probe without electron emission from the probe has also been done in Ref. 6.

Figure 3 shows the probe potential relative to the plasma potential as a function of Debye number δ for a hot, electron emitting probe at space-charge current saturation. It is clear from the figure that even at current-saturation the probe potential does not reach the plasma potential. The probe potential is lower than the plasma potential, so that electrons emitted from the probe are drawn to the plasma. In Fig 3 normalized currents are also shown; plasma ion and electron currents and the electron current emitted from the probe at space-charge current saturation. The results in Fig. 3 are also for argon plasma.

We used the theory of emissive probe for measurements in our Radial Plasma Source (RPS), shown in Fig. 4, which is described in detail in Refs. 1-3. In all the measurements described here the The maximal intensity of the magnetic field in the mid-plane was 130 G and the discharge current was 1.9 A.

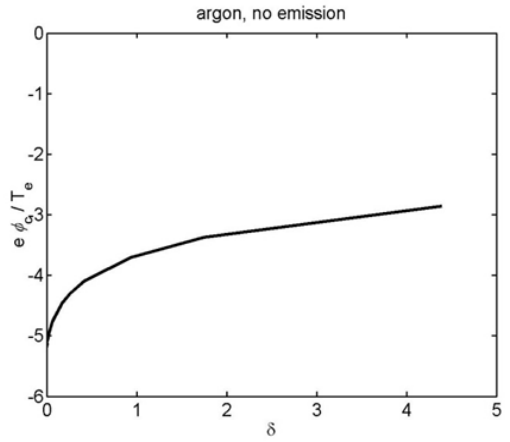

Figure 2. The probe potential relative to the plasma potential versus Debye number: cold probe with no electron emission.

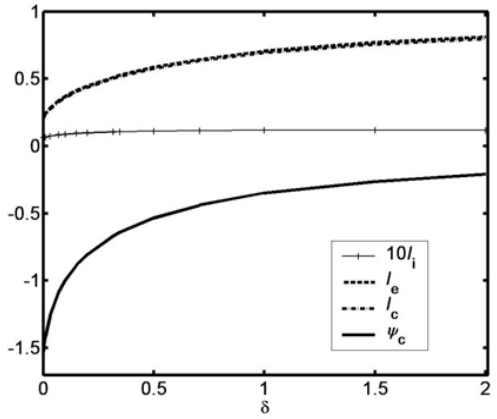

Figure 3. The probe potential relative to the plasma potential versus Debye number: hot electron-emitting probe at space-charge current saturation.

Figure 5 shows probe potential measurements with our emissive probe at various distances from the axis of symmetry of the RPS. At each location shown are measurements for two values of the gas flow rate and for two modes of the probe. In one mode, the probe is cold and does not emit electrons. In the other mode the probe is hot, e we could have used either one of the two measurements shown in Fig 5, either that with a cold probe or the other with the hot probe, to determine the plasma potential at each location. However, since we need two additional

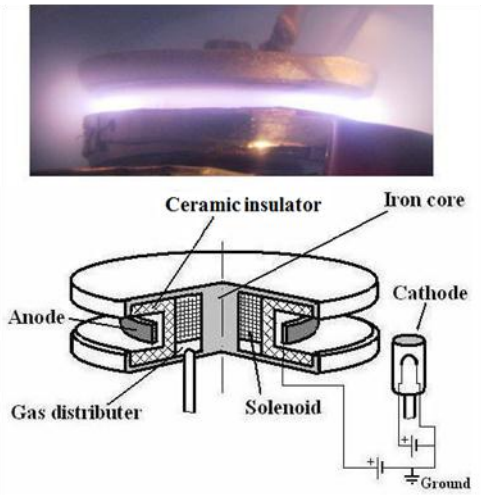

Figure 4. The RPS in operation and a schematic.[1]

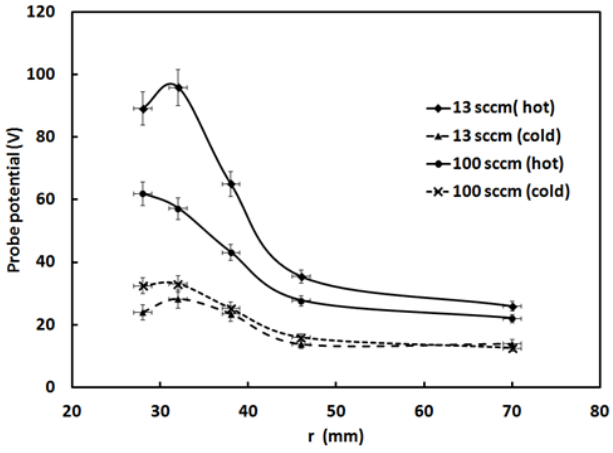

Figure 5. The probe potential in the RPS versus the distance from the axis of symmetry. The cathode is grounded so that its potential is denoted as zero.

parameters, T and δ, in addition to the probe potential, there is one additional piece of data missing. This additional data is the ion saturation current, taken with a Langmuir probe. Figure 6 shows the ion saturation current of a Langmuir probe for the two different gas flow rates at various distances from mits electrons, and is actually at current saturation. Had we known the electron temperature and the Debye number, we could have used either one of the two measurements shown in Fig 5, either that with a cold probe or the other with the hot probe, to determine the plasma potential at each location. However, since we need two additional parameters, T and δ, in addition to the probe potential, there is one additional piece of data missing. This additional data is the ion saturation current, taken

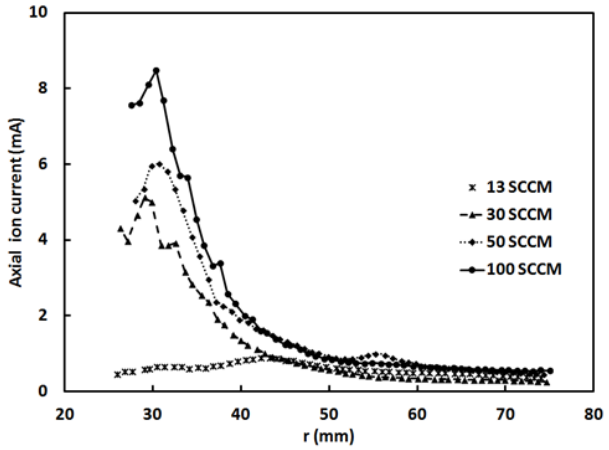

Figure 6. The ion saturation current into a Langmuir probe versus the distance from the axis of symmetry.

with a Langmuir probe. Figure 6 shows the ion saturation current of a Langmuir probe for the four different gas flow rates at various distances from the axis of symmetry.

The measurements shown in Fig 6 were taken with the Langmuir probe which was positioned in the (r,ϑ) plane, so that the plasma flow is parallel to the probe plane. The measurements with the two probes enable us to calculate the distribution of the plasma potential and of the electron density and temperature, as is explained shortly. In the next section we show how we used the data to obtain the plasma parameters.

III. Deducing the plasma parameters

At each location and for each gas flow rate, we look for the plasma potential, the electron temperature, and the plasma density. For these three unknowns, we have three measurements. Let us write the relations:

$$\begin{aligned} e\phi_{plasma} &= e\phi_{probe,cold} + Tf_{cold}(\delta) \\ e\phi_{plasma} &= e\phi_{probe,hot} + Tf_{hot}(\delta) \\ I_{sat} &= \mathbf{0.6}enA\sqrt{T/m_i} \end{aligned} \qquad (1)$$

Here, $\phi_{probe,cold}$, $\phi_{probe,hot}$ and I_{sat} are measured. The functions f_{cold} and f_{hot} are calculated in Figs 2 and 3, A is the area of the Langmuir probe, and δ is a function of the unknowns n (the plasma density) and T. We solved these equations in each location for ϕ_{plasma}, n, T. Until here it is the description of the method, as we have already described before.[6] We now present detailed new results using this method. The radial profiles of the plasma potential, of the plasma density and of the electron temperature are shown in Figs. 7, 8, and 9, respectively. First, in Fig. 7, the calculated plasma potential is shown. Next we show, in Fig. 8, the calculated plasma density. Finally, in Fig. 9, we show the calculated electron temperature. In the next section we discuss the plasma parameters.

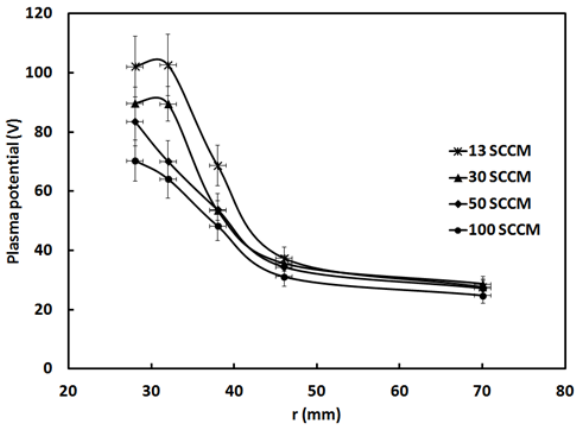

Figure 7. The plasma potential versus the distance from the axis of symmetry for various gas flow rates.

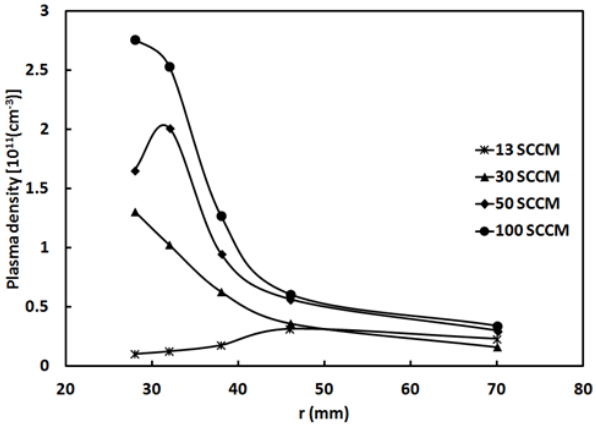

Figure 8. The plasma density versus the distance from the axis of symmetry for various gas flow rates.

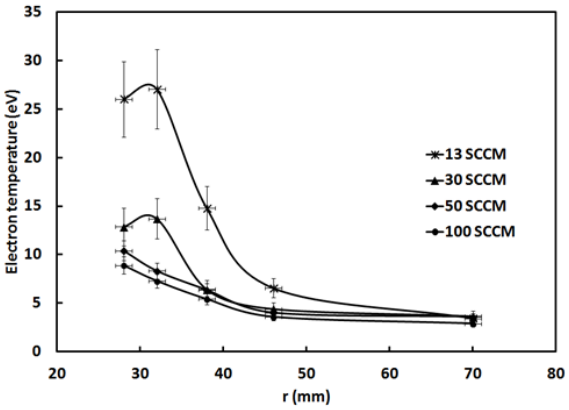

Figure 9. The electron temperature versus the distance from the axis of symmetry for various gas flow rates.

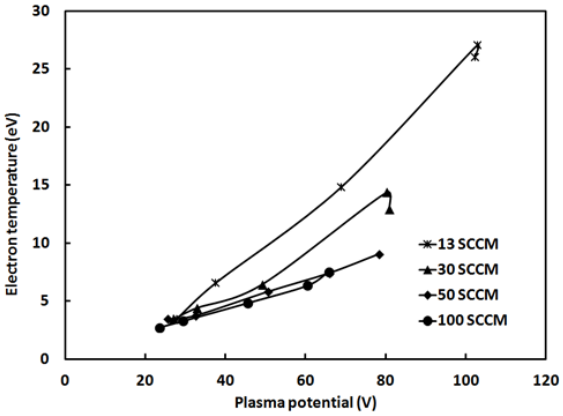

Figure 10. The electron temperature versus the plasma potential for various gas flow rates.

IV. Discussion – the origin of the thrust

From the measurements of the plasma potential and electron temperature, we construct Fig. 10. It is seen in the figure that there is an approximately linear relation between the temperature and the potential, similar to that found for the Hall thruster.[8] The slope for the higher gas flow rates is about 0.1, similar to that found in Ref. 8. However, at the lower gas flow rates, the slope is about 0.2, indicating that electrons losses are smaller so that the electrons reach a higher temperature.

We note that for a higher gas flow rate the plasma density is higher. This is probably due to the smaller ionization mean free path for each electron. For a fixed discharge current (which is mostly electron current), the smaller mean-free-path for ionization results in higher-density plasma.

As the gas flow rate is increased, the plasma density increases while the electron temperature decreases. The plasma pressure increases, as is shown in Fig. 11. The plasma pressure is very small when the gas flow rate is 13 sccm, and is of a similar higher value for the 3 higher gas flow rates.

A question arises as to the relation between the plasma pressure and the force exerted by the ion-neutral flow

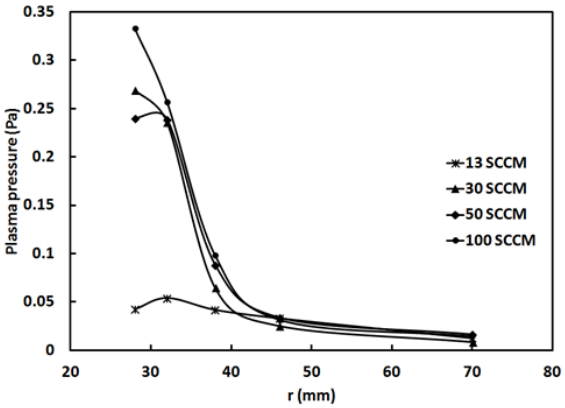

Figure 11. The plasma pressure versus the distance from the axis of symmetry for various gas flow rates.

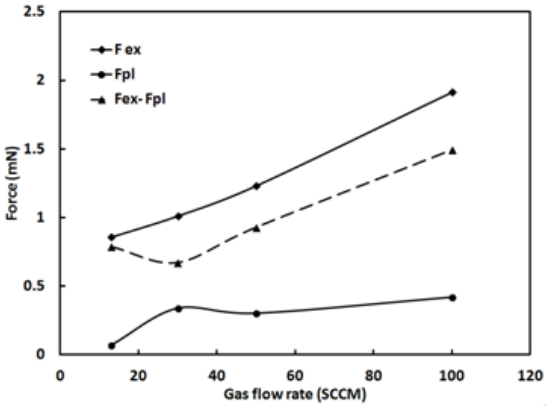

Figure 12. The measured force exerted by the flow, the force estimated by the plasma pressure, and the difference between the two (probably the magnetic force), all versus the gas flow rate.

exiting the RPS. We have performed a comprehensive study of that force.[1-3] Figure 12 shows a comparison of the

size of the total radial force exerted by the flow to the force exerted by the plasma pressure. It is seen in the figure that the force exerted by the flow is considerably larger than that by the plasma pressure. The other force is the magnetic force, and it is larger than the force due to the plasma pressure.

The forces shown in Fig. 12 are calculated as follows. The force by the flow is calculated as Fex = $(F_t - F_g)\times 2\pi r_b/c$. Here, F_t is the total force measured by our balance force meter (BFM),[1-3] F_g is the force exerted by the gas flow immediately after the RPS discharge is turned off, r_b is the distance between the force meter and the axis, and c is the width of the BFM sensing plate. In our experiment r_b = 70 mm and c = 20 mm. The force due to the plasma pressure is estimated as $Fpl = n_0T_0\times 2\pi R_s h$, where n_0 and T_0 are the plasma density and electron temperature at the location of maximal plasma pressure, R_s is the RPS outward radius and h is the width of the acceleration channel (R_s = 40 mm and h = 5 mm).

Another question arises. How comes the magnetic field force is larger for the larger mass flow rate. If the discharge current is maintained constant, then an increase of the mass flow rate is expected to increase the neutral-gas density, and therefore to increase the electron-neutral collision frequency. For a constant magnetic field, the Hall parameter is expected to become smaller, resulting in a smaller azimuthal current and a smaller magnetic field force. The magnetic field force shown in Fig. 12 increases with the increase of the mass flow rate.

We suggest that the path of the electrons from the cathode to the anode changes with changes in the mass flow rate, even if the discharge current is the same. The electron path at the low mass flow rate might be in a region for which the magnetic field force pushes part of the flow onto the wall. When the mass flow rate increases, it could be that the electrons move closer to the midplane, resulting in a larger momentum being delivered to the flow. The details of the cross field transport are not less important than the size of the Hall parameter.

Acknowledgments

This research has been partially supported by the Israel Science Foundation (Grant No. 765/11).

References

[1]G. Makrinich and A. Fruchtman, *Phyics of. Plasmas*, Vol. 16, 2009, pp. 043507-1 - 043507-8.

[2]G. Makrinich and A. Fruchtman, *Applied Physics Letters*, Vol. 95, 2009, pp. 181504-1 - 181504-3.

[3]G. Makrinich and A. Fruchtman, *Phyics of. Plasmas*, Vol. 20, 2013, pp. 043509-1 - 043509-8.

Books

[4]R. S. Sigmond, *Journal of Applied. Physics*, Vol. 53, 1982, pp. 891 – 898.

[5]A. Fruchtman, D. Zoler, and G. Makrinich. Physical Review E, Vol. 84, 2011, pp. 025402(R)-1 - 025402(R)-4.

[6]A. Fruchtman, D. Zoler, and G. Makrinich, "Theory of a cylindrical emissive probe," *Proceedings of the 20th International Symposium on Plasma Chemistry*, Paper 661, (Philadelphia, July 24-29, 2011) (http://www.ispc-conference.org/index.php?option=com_chronocontact&chronoformname=ProceedingsPhiladelphiaSearchPapersResult&Itemid=130&Title=&Author=Fruchtman&Affiliation=).

[7]F. F. Chen and D. Arnush, *Physics of Plasmas*, Vol. 8, 2001, 5051 - ?.

[8]D. Staack, Y. Raitses, and N.J. Fisch, *Applied. Phyics. Leters*, Vol.. 84, 2004, 3028-?.